Available online at www.sciencedirect.com
ScienceDirect
Remote Sensing of Environment 108 (2007) 9–23
Remote Sensing of Environment
www.elsevier.com/locate/rse

Repetitive interpolation: A robust algorithm for DTM generation from Aerial Laser Scanner Data in forested terrain ☆

Andrej Kobler [a,*], Norbert Pfeifer [b], Peter Ogrinc [a], Ljupčo Todorovski [c], Krištof Oštir [d], Sašo Džeroski [c]

[a] Slovenian Forestry Institute, Vecna pot 2, 1000 Ljubljana, Slovenia
[b] Vienna University of Technology, Austria
[c] Jozef Stefan Institute Ljubljana, Slovenia
[d] Scientific Research Centre of the Slovenian Academy of Sciences and Arts, Slovenia

Received 10 October 2005; received in revised form 24 October 2006; accepted 27 October 2006

Abstract

We present a new algorithm for digital terrain model (DTM) generation from an airborne laser scanning point cloud, called repetitive interpolation (REIN). It is especially applicable in steep, forested areas where other filtering algorithms typically have problems distinguishing between ground returns and off-ground points reflected in the vegetation. REIN can produce a DTM either in a vector grid or in a TIN data structure. REIN is applied after an initial filtering, which involves removal of all negative outliers and removal of many, but not necessarily all, off-ground points by some existing filtering algorithm. REIN makes use of the redundancy in the initially filtered point cloud (FPC) in order to mitigate the effect of the residual off-ground points. Multiple independent random samples are taken from the initial FPC. From each sample, ground elevation estimates are interpolated at individual DTM locations. Because the lower bounds of the distributions of the elevation estimates at each DTM location are almost insensitive to positive outliers, the true ground elevations can be approximated by adding the global mean offset to the lower bounds, which is estimated from the data. The random sampling makes REIN unique among the methods of filtering airborne laser data. While other filters behave deterministically, always generating a filter error in special situations, in REIN, because of its random aspects, these errors do not occur in each sample, and typically cancel out in the final computation of DTM elevations. Reduction of processing time by parallelization of REIN is possible. REIN was tested in a test area of 2 hectares, encompassing steep relief covered by mixed forest. An Optech ALTM 1020 lidar was used, with a flying height of 260–300 m above the ground, the beam divergence was 0.3 mrad, and the obtained point cloud density for the last returns was 8.5 m^{-2}. A DTM grid was generated with 1 m horizontal resolution. The root mean square elevation error of the DTM ranged between ±0.16 m and ±0.37 m, depending on REIN sampling rate and number of samples taken, the lowest value achieved with 4 samples and using a 23% sampling rate. The paper also gives a short overview on existing filtering algorithms.

Keywords: Lidar; Airborne laser scanning; Digital terrain modeling; Forest

1. Introduction

Airborne laser scanning (ALS), also termed airborne lidar (Light Detection And Ranging), is one of many laser remote sensing techniques (Measures, 1992). By measuring the round trip time Δt of an emitted laser pulse from the sensor to a reflecting surface and back again, the distance from the sensor to the surface d is determined using the known speed of light c in air: $d = c\ \Delta t/2$. For measuring the topography of the Earth surface from an aircraft, typically an airplane, the position and attitude of the platform have to be known. These parameters are determined with GPS and IMU, Ip et al. (2004). Through periodical deflection of the emitting direction across the flight

☆ The work on this paper was partly performed at alp-S, Centre for Natural Hazard Management, Innsbruck, Austria.

* Corresponding author. Tel.: +386 1 2007835.
E-mail address: andrej.kobler@gozdis.si (A. Kobler).

0034-4257/$ - see front matter © 2006 Elsevier Inc. All rights reserved.
doi:10.1016/j.rse.2006.10.013

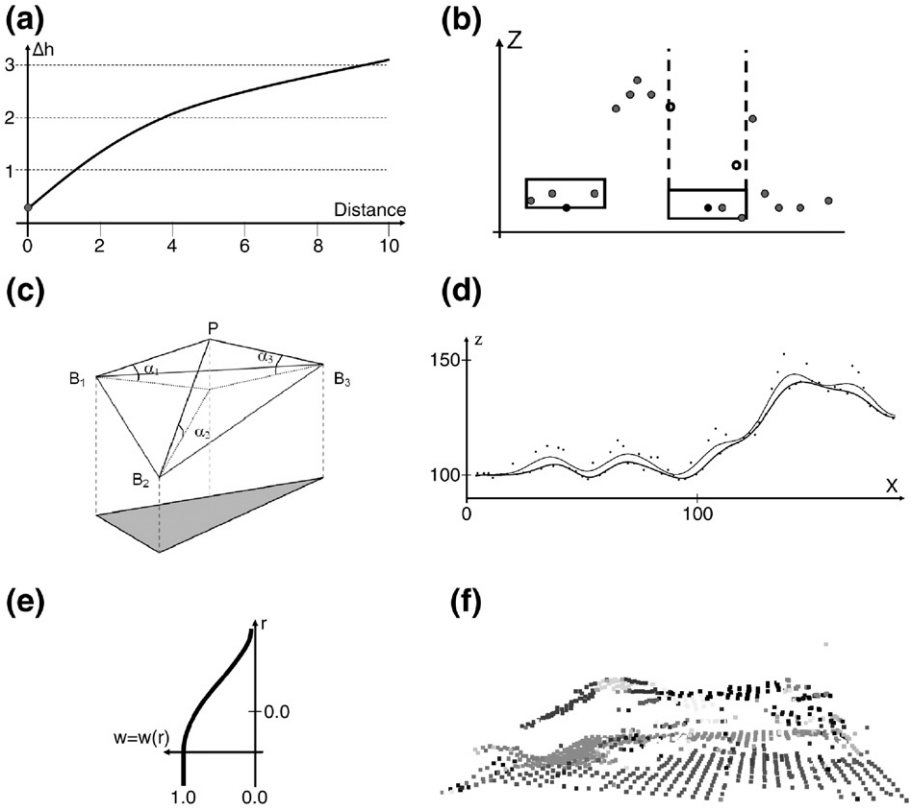

Fig. 1. Filtering of ALS data for ground detection. In (a) the structure element shows the admissible height differences based on distance (units are meters). In (b) a point cloud is shown in a profile with ground, a roof and vegetation points, where at two specific points (black dots) windows are centered. In the right case two points (bold circles) are identified as not-ground points. In (c) a triangle of previously identified ground points (B_1, B_2, B_3) is shown and measures (α_1, α_2, α_3) to determine, if the investigated point (P) shall be classified as ground point. In (d) a first, rough surface model is shown as the upper line computed from the entire point set (profile view) and the lower line shows the DTM in the next iteration. In (e) a weight function is plotted which takes as input the residuals, i.e., the signed distance of the points to the surface. In (f) the segmentation of an ALS pointset is shown in a 3D view with different grey tones for different segments.

path by an oscillating or rotating mirror and by the forward motion of the aircraft, a dense cloud of points is sampled on the Earth's surface in the form of a swath. Multiple flight lines are necessary to cover a large area. Commercial airborne laser scanners can operate from heights up to 5000 m, reach a measurement frequency of 100,000 points per second and higher, and a height accuracy of a few cm. This leads to a typical point density of one point per m^2, but often a higher density is achieved. Lower densities are not untypical either, resulting from large flying heights, from fast fixed wing aircraft operation and low pulse repetition rates.

Airborne laser scanning is different to radar because the footprint of the emitted signal is much smaller, Bufton (1989). Radar measurement therefore cannot provide such a high spatial resolution as laser measurements. With SAR (synthetic aperture radar), and especially InSAR (interferometric SAR) resolution can be increased, but the accuracy of laser measurements is not reached (Andersen et al., 2004). A laser shot can penetrate the tree crowns, i.e., look through small gaps in the foliage, and reach the ground. Therefore, the distance to the ground below trees can be measured. Passive optical remote sensing techniques for inferring terrain elevation, i.e., photogrammetry, require that (1) enough sun light is scattered back from one ground position onto (2) two images, which makes the measurement of ground below canopy elevation from imagery almost impossible (Kraus & Pfeifer, 1998).

Because of its immediate generation of 3D data, high spatial resolution and accuracy, ALS data is becoming popular for the reconstruction of digital terrain models (DTM; Sithole & Vosselman, 2004) and virtual city models (Kaartinen et al., 2005). Since the lidar signal has the ability to pass through gaps in foliage and reflect from different parts of trees it is also used for measuring tree height and estimating other forest stand parameters (Hyyppä et al., 2004).

The backscattering mechanism utilized in airborne laser scanning is diffuse reflection. The (laser) light coming from one direction (i.e., from the sensor) is scattered at the reflecting surface into all directions. A small portion of the emitted energy therefore travels back to the sensor where the runtime is measured. As the diameter of the laser pulse is not infinitely small but has a certain footprint, typically in the range of 50 cm to 1 m, several objects can be the source of the backscattered signal. Modern receivers can record multiple echoes, e.g., the first, second, third, and last

echo. These discrete return small footprint systems have to be distinguished from the systems recording the entire backscattered waveform (Wagner et al., 2006), and large footprint systems as, e.g., NASA's Vegetation Canopy Lidar (VCL; Blair et al., 1999), and GLAS (Zwally et al., 2002), instruments. Therefore, ALS provides points measured on objects between the sensor and the ground surface, depending on where the laser beam is reflected. As it can be reflected by power lines, vegetation leaves, house roofs, etc., many points do not lie on the ground surface. Classification of these points into ground and object (off-terrain) points is called *filtering*. This is an essential step necessary for digital terrain model (DTM) generation, but also for further reconstruction of topographic features (houses, power-lines, etc.) that is often performed relative to the DTM, using a normalized surface model.

Due to multi-path reflection, points which apparently lie below the Earth's surface, can also be obtained. If a portion of the emitted energy travels from the sensor to the ground surface and not immediately back to the receiver but bounces to another surface before, the runtime measured corresponds to a distance which is longer than the platform ground distance and the point position will be computed below the ground.

As the filtering methods operate purely in an automated mode, i.e., with one set of parameters for large areas (typically several km^2 to several hundreds of km^2) the resulting DTMs are not optimal in all areas, requiring interactive fashions of parameter testing and manual correction of the results. Steep wooded terrain is especially considered as a problem in filtering. Therefore, there is a tangible need for precise terrain information in difficult relief. Within this paper we present a new filtering algorithm for steep relief under dense forest cover, where other filtering algorithms typically have problems distinguishing between ground returns and points reflected in the vegetation. The algorithm is also new in the sense that it cannot be put into any one of the four main categories specified in Section 2. On one hand it is able to deal with sparse ground returns under dense forest canopy, but on the other hand also with highly redundant ground returns in forest openings. The problem of negative outliers, originating from multi path reflections, is also addressed by this new algorithm.

The motivation for our work was to get high quality terrain elevations as basis for further forestry related analysis of lidar data. The specific contribution of this work is a method which provides a precise and reliable DTM even if the laser scanner ground hits are sparse and very irregularly distributed. Variation in the number of ground hits may vary on all scales as it is affected by vegetation type, terrain characteristics, and scanner characteristics. The portion of points on the grounds is affected by the vegetation, where different tree species lead to different penetration rates, and by the sampling pattern of the laser sensor, which does not necessarily lead to equal point postings on the ground. This results in higher and lower point densities, respectively, within one swath. Depending on the airborne laser scanner in use, the point density becomes higher (oscillating mirror) or lower (rotating mirror) at the sides of the swath.

Section 2 of this paper summarizes the existing methods of filtering, Section 3 illustrates and explains in detail the new filtering algorithm, in Section 4 the test area and the input data are described, Section 5 lists and discusses the algorithm results for the test area, and finally, Section 6 draws the conclusions.

2. The state of the art in lidar filtering

Different concepts for filtering have been proposed so far. The first group of filters got its name from mathematical morphology (Haralick & Shapiro, 1992) and is used in morphological filtering (Vosselman, 2000). A structure element, describing admissible height differences depending on horizontal distance is used (Fig. 1a). The smaller the distance between a ground point and its neighboring points, the less height difference is accepted between them. This structure element is placed at each point so off-terrain points are identified as those above the admissible height difference. The structure element itself could be determined from terrain training data resulting in an optimal structure element to minimize type I and type II errors, or it could be obtained from maximum terrain slope assumptions. Variants of the morphological filtering are described by Sithole (2001), where the structure element depends on terrain shape. For steeper areas higher admissible height differences are allowed. The steepness itself is determined in an averaging procedure over large areas. A similar idea is presented by Zakšek and Pfeifer (2006) where the structure element is inclined as a whole in order to follow the terrain, i.e., the rotational symmetry around the z-axis is lost. The reason is that height differences downwards have different characteristics compared to the upwards height differences, which is not considered in the other morphological filters. Kilian et al. (1996) use multiple structure elements of different size in the morphological operation Opening. This method works on a rasterized dataset, whereas the previous methods work on the point cloud directly. With different structure element (window) sizes, different objects (small cars, big buildings) are tackled. Weights are assigned to the points depending on the window size, which are finally used for the classification. Zhang et al. (2003) describe a comparable method using different window sizes and allowed height differences within each window (Fig. 1b), especially providing a method for choosing these parameters. Lohmann et al. (2000) apply Erosion and Dilation to replace raster terrain elevations with the filtered elevations.

The second group of filters works progressively, where more and more points are classified as ground points. Axelsson (2000) uses the lowest points in large grid cells as the first ground points and a triangulation of the ground points identified so far as reference surface. For each triangle one additional ground point is determined by investigating the offsets of the unclassified points in each triangle with the reference surface (Fig. 1c). The offsets are the angles between the triangle face and the edges from the triangle vertices to the new point. If a point is found with offsets below threshold values, it is classified as a ground point and the algorithm proceeds with the

next triangle. In this way the triangulation is progressively densified. von Hansen and Voegtle (1999) describe a similar method with a different choice of starting points (lower part of the convex hull of the point sets) and different offset measures. In the work by Sohn and Dowman (2002) the progressive densification works first with a downward step, where points below the current triangulation are added, followed by the upward step, where one or more points above each triangle are added.

The third group of algorithms is based on a surface model through the entire point set that iteratively approaches the ground surface. A first surface model is used to calculate residuals from this surface model to the points (Fig. 1d). If the measured points lie above it, they have less influence on the shape of the surface in the next iteration, and vice versa (Fig. 1e). Kraus and Pfeifer (1998) use linear prediction, i.e., simple kriging, with individual point accuracies (i.e., nugget components in the variogram), as a surface model and a weight function from robust adjustment to compute weights based on the residuals. Points with high weights have small nugget components and therefore more influence on the run of the surface, while points with small weights have large nugget components and correspondingly less influence. In the work by Pfeifer et al. (2001) this method has been embedded in a hierarchical approach to handle large buildings and reduce computation time. Elmqvist (2001), Kass et al. (1988) use a snake-approach, where the inner forces of the surface determine its stiffness and the external forces are a negative gravity. Iteration starts with a horizontal surface below all points that moves upwards to reach the point, but inner stiffness prevents it from reaching up to the points on vegetation or house roofs.

Finally, the fourth group of filters works on segments (Fig. 1f). Sithole (2005) describes a method that classifies the segments based on neighborhood height differences. Nardinocchi et al. (2003) apply a region growing technique based on height differences to get segments. The geometric and topologic description of the regions can be presented with two graphs, whereupon a set of rules is applied to produce a further segmentation, where the segments are classified into three main classes: terrain, buildings, and vegetation. Jacobsen and Lohmann (2003) use the eCognition software on gridded data, and segments are obtained from region growing. Amongst other criteria they apply the compactness of these segments and the height difference to the neighboring segments, in order to detect different types of areas including terrain. In the work of Schiewe (2001) maximum and average gradients are used for classification of the data. These methods work on larger entities, i.e., not on the single points or pixels, and are therefore less influenced by noise. This is demonstrated in Fig. 1f, showing two large segments for the ground, one in the foreground and one in the back, a couple of segments for the roofs of the two connected houses, and many single or few point segments for the points on the vegetation.

An experimental comparison of the performance of some filter algorithms is described by Sithole and Vosselman (2004). The fourth group of algorithms, i.e., the segmentation based algorithms, has its advantage in areas where distinct segments are found, i.e., areas influenced strongly by human (building) activities. In wooded areas this does not hold, but also the other algorithms presented tend to fail, especially because the point cloud in steep terrain has – looking at a local neighborhood – similar characteristics as vegetation: large height differences at small horizontal distances.

3. The REIN algorithm

The presented method is intended to generate a DTM in steep relief covered by heterogeneous forests, which leads to a high variation in the penetration rate and therefore high variation in the number of ground returns per unit area. In flat terrain with sparse forest cover, allowing high penetration rates and a high density of ground returns, the existing filtering algorithms are accurate and efficient. However, filtering results get less accurate in steep relief under dense forest cover. This is partly owed to the larger errors before filtering, due to a decrease in the signal to noise ratio of the backscatter as typically only a part of the emitted energy hits the ground, and due to horizontal errors propagated to the vertical in sloped terrain. However, also because of the presence of low vegetation and understorey, and a possibly reduced point density, compared to open areas, many more classifications as "non-ground point" have to be made by the filter, increasing the uncertainty of the "ground" classification. For such circumstances, we propose a two-stage method that can be summarized as follows:

1. In the initial filtering stage negative outliers and most, but not necessarily all, off-ground returns (positive outliers) are removed. To achieve the latter we use filter algorithms similar to existing techniques as, e.g., morphological filters.
2. In the final filtering and DTM generation stage the DTM is produced from the initially filtered point cloud. For this task, we propose a new algorithm which is able to deal with a partially filtered point cloud in steep relief. The filter was named REIN, for REpetitive INterpolation, because it makes use of multiple ground elevation estimates at individual DTM points in a vector grid or a TIN (Triangulated Irregular Network), interpolated from surrounding ground returns. These elevation estimates are generated from multiple independent samples taken from the initially filtered point cloud. In this paper TINs are used for computing the elevation of the DTM points. Instead of TINs however, any suitable spatial interpolation method could be used for computing elevations at DTM points.

The initial filtering stage is necessary because there are two preconditions for the REIN algorithm to generate DTMs with no or only a few filter errors[1]. The first precondition is that many, but not necessarily all, off-ground returns are removed

[1] While these conditions are necessary, no proof will be given in this paper, that they are sufficient.

from the point cloud before applying REIN. The second precondition is that no negative outliers remain in the point cloud before moving on into the second, final filtering stage. The initial filtering stage has two steps.

The first step is to remove the extreme negative outliers from the point cloud. For each point in the point cloud, we compute its vertical displacement D to the average elevation of its k neighboring points (neighborhood being considered in the X–Y plane). We then rank all the points according to D and discard P percent of points having the largest negative D values. P should be small, but at the same time it must be large enough to ensure no significant negative outliers are retained, even at the cost of removing some non-outliers.

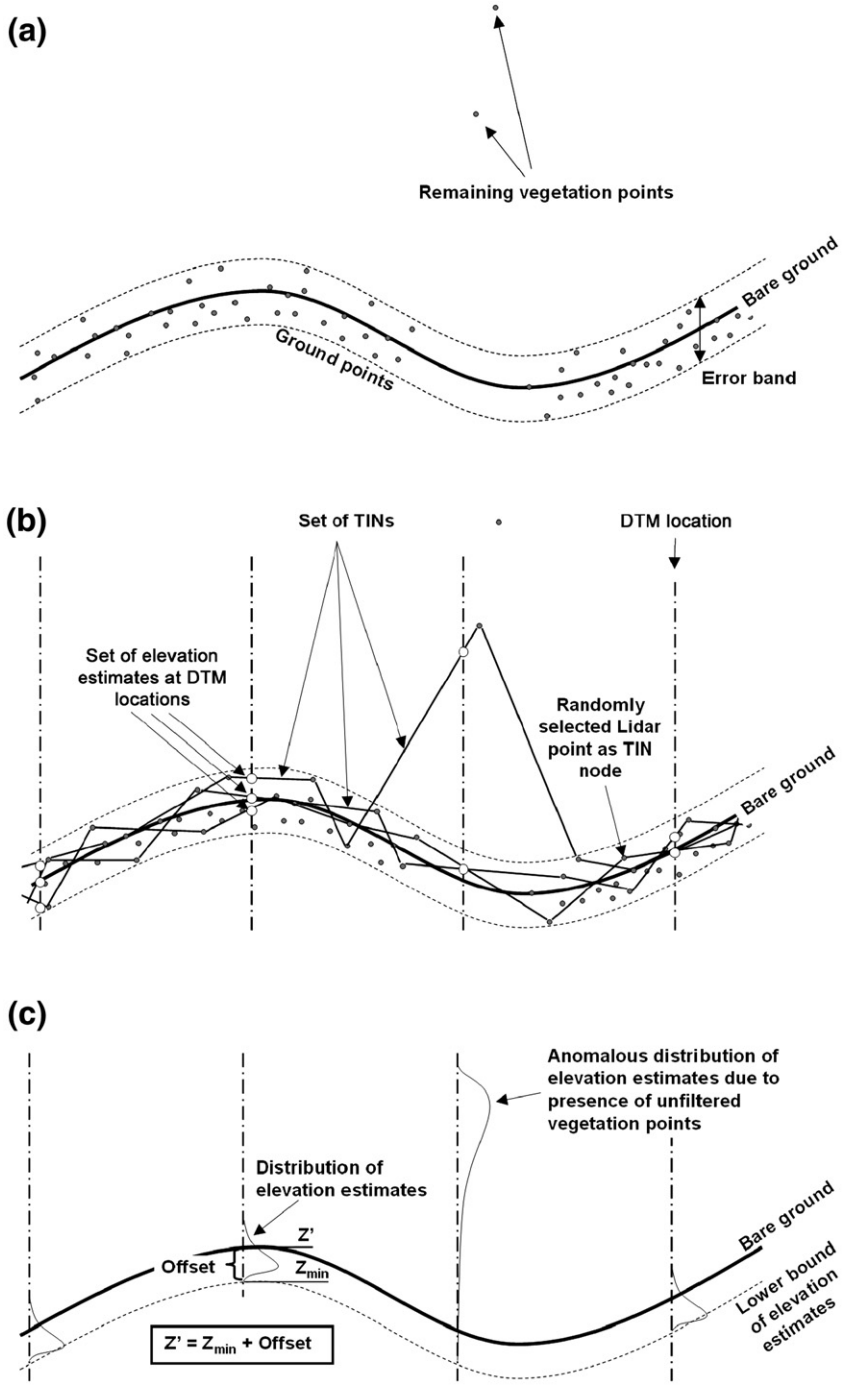

Fig. 2. Illustration of the REIN algorithm used in the final stage of the filtering. (a) The result of the initial filtering stage (using, e.g., a slope threshold filter) are ground points with few remaining unfiltered vegetation points and no negative outliers. Note the redundancy of ground points within the error band. The scattering within the error band is caused by measurement errors, grass and low herbal vegetation. (b) Repeated random selections of lidar points are used to build a set of TINs, out of which sets of elevation estimates are interpolated at the locations of DTM grid points. Note that also the remaining unfiltered vegetation points may become TIN nodes. (c) DTM elevations are approximated by adding global mean offset to the lower bounds of elevation distributions, which are unaffected by the unfiltered vegetation points.

During the second step of the initial filtering stage we remove most off-ground points, using a filter based on the slope between neighboring points. Starting from the lowest point, for each point its k nearest neighbors are investigated, and if the slope between a point pair is larger than a threshold the higher of the two point is removed. The slope threshold is set to a slightly higher value than the steepest slope expected in the area of interest. This prevents accidentally filtering out the ground points in steep areas; however more off-ground points remain in the point set as a consequence and have to be dealt with in the final filtering and DTM generation stage.

The input for the final filtering and DTM generation stage is thus a filtered point cloud (FPC) containing mostly ground points scattered within the error band, with some positive and no negative outliers. The error band is the buffer zone along the surface of the true bare ground (Fig. 2a), caused by the lidar point errors due to the lidar range measurement errors, scanning angle error, direct geo-referencing error and grass and low herbal vegetation. Another component affecting this error band is caused by relief details with extent below the lidar sampling distance which therefore cannot be recovered. Because the steep relief imposes a high threshold used in the slope filter, some positive outliers, i.e., vegetation points (Fig. 2a) remain in the initially filtered point cloud. These outliers would introduce errors into the DTM, if it were generated directly from FPC. Instead of this, a DTM is fitted to the ground points within the error band using the REIN algorithm.

The basic idea of the REIN algorithm (illustrated in Fig. 2, pseudo-code in Appendix A) is to make use of the redundancy in the initially filtered point cloud in order to mitigate the effect of the residual off-ground points in the FPC. The true elevations at those locations in the X–Y plane, that we want to include into the DTM (termed DTM locations), can be approximated from repeated independent estimates of the relief. Each estimate is based on an independent random sample (termed FPC_s) taken from the FPC. During each iteration the points of each FPC_s are used as nodes to build a triangulated irregular network (TIN). Elevations at DTM locations are interpolated from each triangulated irregular network (Fig. 2b). As mentioned before, any spatial interpolation method could be used instead of a TIN. Note that the DTM locations could be distributed either systematically (as in a DTM grid) or irregularly (as in a TIN). After repeating the interpolation a number of times we get a distribution of elevation estimates at each DTM location. The true elevations can be estimated, based on two observations:

1. The lower bounds of the distributions are almost insensitive to positive outliers. On the other hand, the negative outliers have no effect, assuming they were removed previously. This means that, within comparable forest and relief circumstances, the lower bounds have a more or less constant vertical offset to the true bare-ground surface (Fig. 2b, c). Comparable forest circumstances mean a limited variation in laser penetration rates throughout the area of interest, enabling a more or less consistent efficiency of vegetation point removal in the initial filtering stage. Comparable relief circumstances mean there is a limited variation in relief coarseness.
2. The majority of the distribution bounds match the error band, assuming that (a) the sampling rates to collect FPC_s were not too low and (b) relatively few positive outliers remained in the FPC. The assumption (a) implies that only rarely elevation interpolations would smooth out the relief curvature between sampled points, while the assumption (b) implies that only a few distributions have anomalous upper bounds (Fig. 2c). Further assuming that the width of the error band is constant within comparable forest and relief circumstances, we can estimate the global mean offset between the lower distribution bounds and the true relief elevations (gmo). The gmo equals the average of differences $d_{ij}=z_{ij}-z_{j,\min}$ over all DTM locations, where z_{ij} is the i-th elevation estimate at the j-th DTM location and $z_{j,\min}$ is the lowest elevation estimate at the j-th DTM location.

After computing gmo and all the $z_{j,\min}$, the estimate of the true elevation z_j at the j-th DTM location is:

$$z_j = z_{j,\min} + \text{gmo} \tag{1}$$

In Eq. (1) gmo is a quantity computed from all z_{ij}, thus robust, and $z_{j,\min}$ and therefore also z_j are values for one DTM location. Note that simply drawing a random sample out of the available ground points during each iteration of REIN would yield TINs that are overly detailed in areas of high point density and too generalized in areas of low point density. Such irregularities are caused by variable penetration rates in a heterogeneous forests and by irregularly spaced scan-lines. It is therefore important that each sample of points used as TIN nodes should be spatially as unbiased as possible. This is ensured by a selection procedure, where a set of random locations in X–Y plane is generated within the bounds of the filtered point cloud and then the nearest point found for each random location is chosen. Thus the sparse lidar ground returns under very dense forest canopy have higher chance of being selected than the more frequent ground returns in less dense forest stands, enabling REIN to give more consistent results irrespective of canopy cover.

The operation of REIN is guided by two parameters — *samplesize* (the number of points in each FPC_s) and *numsamples* (the number of iterations). Both parameters influence the quality of the DTM and their effect will be assessed in Section 5.

Appendix A states the REIN algorithm and the selection procedure in detail. The REIN algorithm was implemented in the object-oriented Python language due to the ease of programming. The Python's efficient Numarray library was used for all computations involving grid of DTM locations. The triangulation of the sampled lidar points was done by integrating an existing implementation of a 2D Delaunay triangulator called Triangle (Shewchuk, 2005). Since lidar

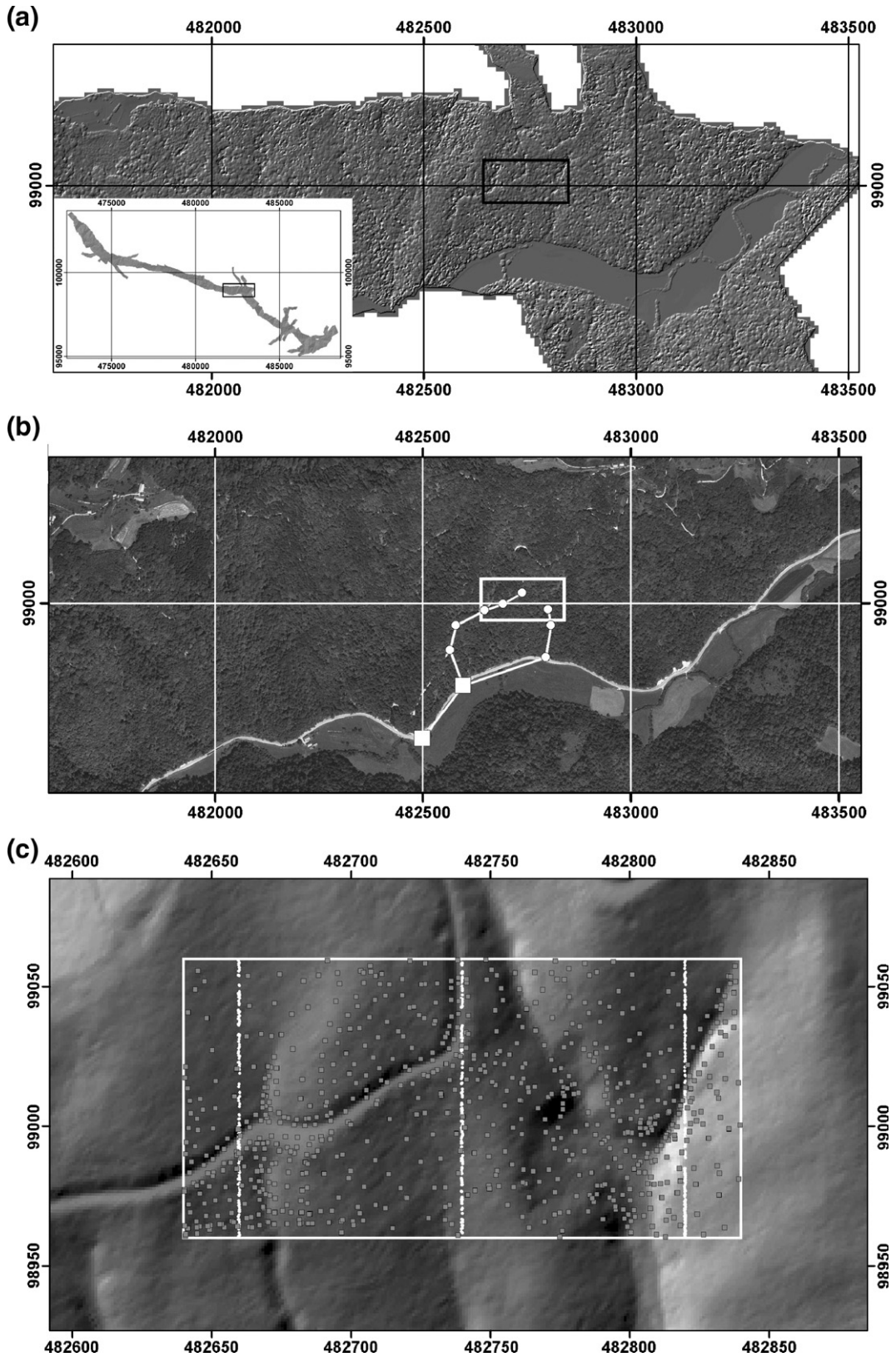

Fig. 3. In (a) and (b) the test site and its surroundings are shown as a DSM of lidar points and in an aerial orthophoto, respectively. The area is covered with *Pinus sylvestris* and *Castanea sativa* mixed forest on steep terrain in central Slovenia. The inset in lower left of (a) presents the DSM of the entire project area. The embedded rectangles in (a) and (b) represent the location of test area. In (b) also the location of the GPS points (white squares) and the total station transects (circles), measured for field validation, are shown. In (c) the filtered DTM of the test area is shown (white rectangle), where the three North–South transects contain the visually identified ground points and the scattered points, that were measured by a total station. The middle profile is shown in (d). Points that are classified as vegetation in the visual identification are shown as black dots, ground points as circles. The DTM computed by the proposed algorithm is shown as black line.

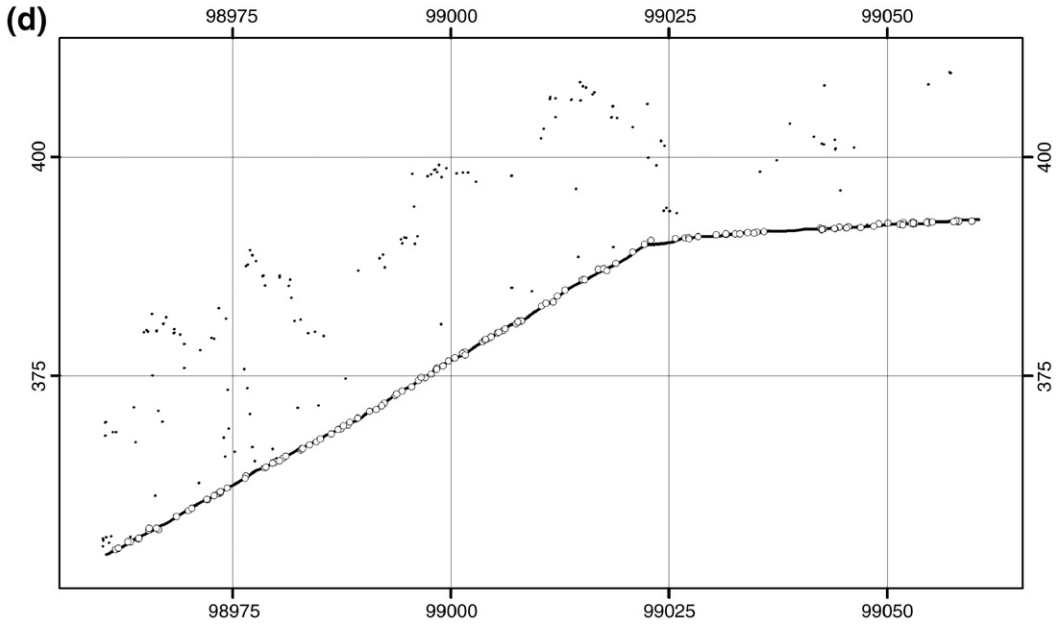

Fig. 3 (*continued*).

datasets are usually massive, using some spatial indexing setup instead of flat lists of points is important to manage the datasets efficiently. In our implementation we stored the point cloud in the quadtree data structure for efficient point indexing (Samet, 1984). The distance ranking method (Hjaltason & Samet, 1995) was used to find the n nearest neighbors in a quadtree. During the initial filtering stage (slope filtering) and during repeated sampling of the initially filtered point cloud, spatial indexing and quick search of points turned out to be essential for ensuring a reasonable processing time.

4. Test data and area description

We assessed the performance of the REIN algorithm in a test area of steep forested relief in central Slovenia. Fig. 3a shows a DSM covering a test area of 2 ha, which represents 0.17% of the total area scanned (1179 ha). In Fig. 3b an orthophoto of the area is shown. The project area was scanned for a power line company on April 30, 2003, when the vegetation was almost fully developed. From the final results (see Section 5) the penetration rate estimated for the last echoes recorded is 47%.[2] The data acquisition was done in the first and last mode with an Optech ALTM 1020 scanning Lidar, mounted onto a helicopter. The flying height was 260–300 m above the ground, with a ground speed of 25–50 km/h, and a beam divergence of 0.3 mrad[3]. The obtained point cloud density was 6.4 m^{-2} and 8.5 m^{-2} for first and last returns, respectively. This value is higher than obtained by many missions so far[4], where a typical density is 1 m^{-2}. Only the last returns were used to generate the DTM. While the flying height was rather low, it was counterweighted by a low pulse repetition frequency (20 kHz) considering that currently available systems offer pulse repetition frequency values between 66 kHz and 150 kHz. The specifications of the instrument state that the vertical measurement accuracy is ±15cm, and the horizontal accuracy ±35cm in either direction for the given flying height. If the error is only looked at in the vertical direction, then for a 45° slope this adds up, by addition of variances, to ±38 cm.

The average terrain slope of the test area was 30°, while the slopes along the forest road embankment and in the erosion dykes reached up to 70°. The test area is covered with a mixed forest with 18 m average tree height, estimated from a normalized digital surface model. The main species are *Pinus sylvestris* and *Castanea sativa* in the tree layer, and *Fagus sylvatica* and *Rhamnus frangula* in the forest understorey. In the herbaceous layer *Pteridium aquilinum* covers half of forest floor and there is continuous cover of *Vaccinium myrtillus* underneath. The average forest canopy cover is 0.67 with extreme values up to 0.86. Canopy cover was estimated for circular plots (r=5 m) centered at reference ground points as the proportion of first and last lidar returns higher than 1 m above ground versus all first and last lidar returns.

From the point cloud of last returns, ground points (N=563) for estimation of DTM quality were visually identified within 3

[2] The selected ground points were used for building a DTM and all points less than 0.5 m above that surface are considered to be ground points.

[3] This, and considering the beam diameter at the aperture, implies a laser footprint diameter of ~20 cm, which is lower than typically obtained values of 50–100 cm.

[4] However, due the appearance of higher frequency instruments (150 kHz at the time of writing), equal or higher point densities can be expected in future applications.

systematically placed transects oriented in North–South direction, each transect being 0.5 m wide and 100 m long (Fig. 3c). To distinguish the ground points each transect was interactively rotated. The manual filtering could be seen as the best possible classification into ground and off-terrain points given no additional information. Sithole and Vosselman (2004) suggested this method for their comparison of filter algorithms. Practice has shown that filter errors are often obvious to humans. Correspondingly visual check and correction are routinely performed by data providers for classification. As example, the visual identification within the middle transect is shown in Fig. 3d.

For overall performance evaluation, a total number of 744 field measured ground points (Fig. 3c) were measured with a total station Leica TC605L. Two points were measured with GPS and from these points transects were established for measuring ground heights below the canopy cover. Applying error propagation, the accuracy of these points is estimated as ±5 cm in either coordinate direction. Converting these values into a height error only using a 45° slope as before, the height error amounts to ±9 cm.

All the data is projected in the current Slovenian coordinate system that is based on the Bessel ellipsoid 1841 and Gauss–Krüger rectangular plane coordinates (conformal, transverse

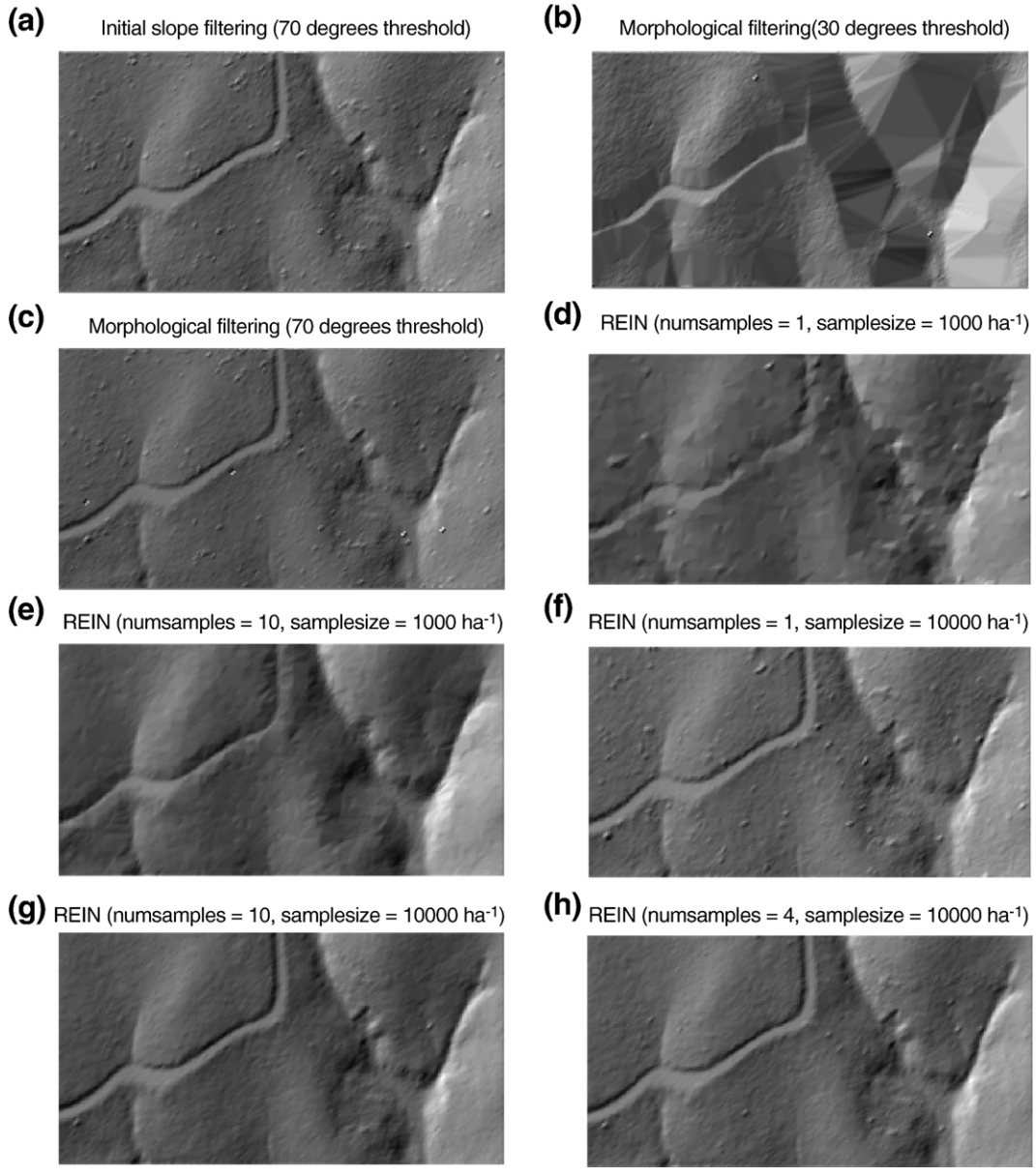

Fig. 4. Comparison of the shaded relief images of the slope filtered baseline DTM (a), morphologicaly filtered DTM (b and c), and results of REIN filtering (d–h). All DTMs have 1 m by 1 m horizontal resolution. Note the effects of extreme values of REIN parameters: low samplesize values cause relief generalization (d, e) and low numsamples values cause artifacts due to remaining unfiltered vegetation (d, f). High numsamples and high samplesize values yield fewest artifacts (g), however high samplesize with moderate numsamples (h) yields marginally better RMSE and saves computation time.

cylindrical projection). The projection is Transverse Mercator with a central meridian of 15° east, latitude origin 0°, a scale factor of 0.9999, false easting of +500,000 m, and false northing of −5,000,000 m.

5. Results and discussion

In this section the computation of the DTM is described and an evaluation of the method is performed in several ways. A visual analysis is performed to check for obvious filter errors or other artifacts of the algorithm and a comparison to the visually filtered subset (as described in Section 4) of the original point cloud is performed. Additionally, the REIN results are compared to the results of another filter algorithm, and finally, the REIN results are compared to the field measured ground points. Each of these evaluations highlights different aspects of the quality assessment as detailed below. First, however, the computation of the DTM by means of REIN and the choice of parameters is described.

5.1. Parameter selection and visual analysis

The visually identified points were used to select the optimal parameters for the DTM computation. The advantage of this reference data set is, that it is not subjected to georeferencing or calibration errors, neither from the LRF, Scanner, GPS, and IMU sensor system, nor from errors in the combination of GPS and the total station measurements. Also different concepts of the actual ground elevation, i.e. top of the herbaceous vegetation, soil–air interface, or a value in between, measured by different devices does not come into play. The only uncertainty stems from the visual interpretation, but as experience has shown, human operators are reliable in distinguishing between ground and vegetation hits, as described in Section 4.

All the DTM grids generated in this study have a horizontal resolution of 1 m by 1 m. First a baseline DTM was generated from the last returns, by removal of negative outliers from the original point cloud, followed by slope filtering. The optimal k and P values for removing negative outliers were determined experimentally and finally set to 10 and 0.2%, respectively. The mean of all average height differences from a point to its 10 nearest neighbors amounts to −0.1 m with a standard deviation of ±7 m. The extreme values are, with either sign, 27 m, which is well above the average tree height (18 m, see Section 4). The average vertical distance from the 0.2% deleted points to their 10 nearest neighbors amounts to 17.5 m. With the average tree it cannot be guaranteed, that only negative outliers were removed. Some ground points may have been deleted, provided their 10 nearest neighbors are on average 17.5 m higher.

The slope threshold for the initial filter was set to 70°, which is the steepest slope observed in the test area. This guaranteed that no ground point was removed from the dataset. Fig. 4a shows this baseline DTM. The point density of last returns thus decreased from 8.5 m^{-2} for all last returns to 4.3 m^{-2} in the initially filtered point set. All the points in the initially filtered point cloud were used as nodes to build a TIN from which the regular grid DTM was computed. Using the field-measured ground points the baseline RMSE is ±0.30 m. However, looking at Fig. 4a it is apparent that the result is entirely unsatisfactory. Many off-terrain points are contained in the ground data set, showing up as small hills in the shaded relief view. Comparison with the visually identified ground points gives an RMSE of ±0.13 m, which is too optimistic. The artifacts are not well represented in that figure. The measured field points, on the other hand, are spread more evenly and show a higher error.

The initially filtered point set is identical with the FPC used subsequently by REIN. The quality of the DTM depends on the values of *samplesize* and *numsamples*. The DTM quality indicator was the global root mean square elevation error (RMSE) using the visually identified points. The influence of both parameters on RMSE was determined within the test area: *samplesize* was set to values between 1000 and 10,000 in steps of 1000 points per hectare, and *numsamples* was set to 1, 2,..., 10 iterations (see Fig. 4d–h). Since REIN uses

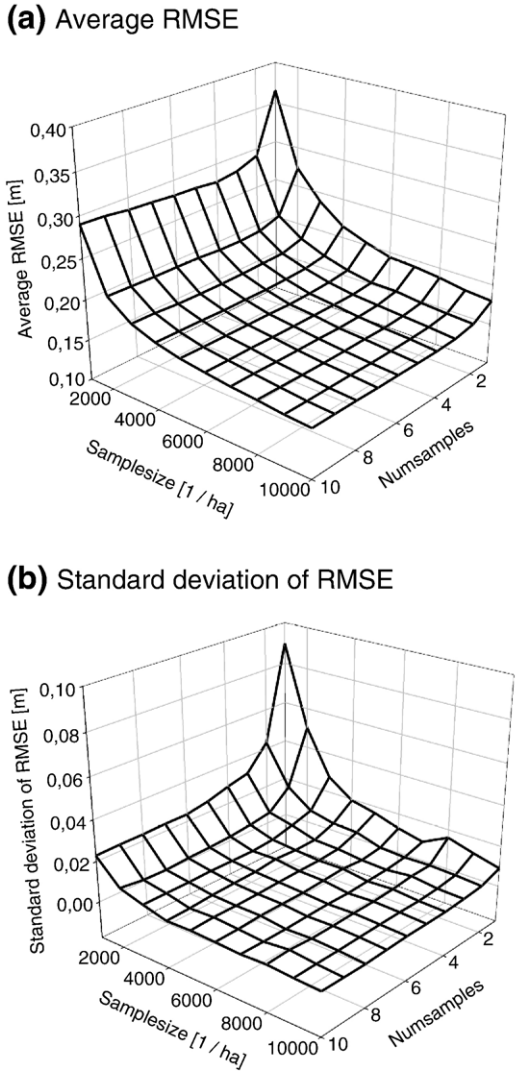

Fig. 5. (a) Influence of the REIN parameters *numsamples* and *samplesize* on the quality of the DTM according to the average RMSE. The average RMSE was obtained by averaging RMSE values of 50 runs of REIN for each parameter combination. (b) Stability of REIN results as indicated by the standard deviation of RMSE based on 50 runs of REIN for each parameter combination.

random sampling of FPC_s in each iteration, the resulting DTM fluctuates between individual REIN runs. Therefore 50 runs of REIN were performed in the test area for each set of REIN parameters and the average RMSE values were computed, based on the two sets of ground points — the field-measured ground points and the visually identified ground points. While the RMSE was only computed for the test area itself, during filtering a 10 m buffer zone was added around the test area, in order to exclude the border effects on the performance of repetitive TIN interpolation.

For selecting the appropriate parameters an analysis based on the visually filtered point cloud ($N=563$) was performed. This assessment evaluates filtering accuracy alone, i.e., not taking the measurement noise of the various components of an airborne scanning lidar into account. Especially errors of georeferencing in the laser data, or any reference data source, do not distort the assessment of filtering accuracy.

From the 50 REIN based DTMs for each parameter combination the obtained average RMSE values, with reference to the visually filtered points, range between ±0.16 m and ±0.37 m (Fig. 5a). The standard deviation of the RMSE ranges between ±3 mm and ±90 mm (Fig. 5b). Fig. 5a shows that increasing the *samplesize* improves the average RMSE, especially at low *samplesize* values. The lowest RMSE value of ±16 cm was achieved with a *samplesize* of 10,000 points ha^{-1} taken from the initial FPC, which means that the sampling rate was 23%. Depending on the *samplesize* REIN needs only 3 to 5 iterations (*numsamples* parameter) to get the optimal RMSE. Further iterations yield a smoother DTM with less artifacts due to unfiltered vegetation, however, the RMSE starts increasing slightly (Fig. 4g and h).

Fig. 4 shows the filtering effect of REIN in comparison with the baseline DTM and with the morphologically filtered DTM. A high level of noise in the baseline DTM (Fig. 4a) and in the morphologically filtered DTM (Fig. 4c) is due to off-ground points because of the high slope threshold, which was used in the slope based filtering and in the morphological filtering. REIN with a very low *samplesize* value in Fig. 4d and e (1000 ha^{-1}, corresponding to a sampling rate of 2%) removed all the artifacts seen in Fig. 4a, but caused over-generalization of relief features. On the other hand, REIN with a high *samplesize* value in Fig. 4g (10,000 ha^{-1}) removed most artifacts while retaining the relief detail as can be seen at the valley lines and road embankments. Based on RMSE and on a visual DTM check the values of *numsamples* used in Fig. 4h (i.e., 4) was found to be optimal (Fig. 5a) for the respective *samplesize* value in the given test area. A low value of *numsamples*, which seems to be optimal in the test area, implies a faster processing. On the other hand, larger fluctuations of DTM quality may be expected due to the random nature of REIN. Fig. 5b confirms this by showing a higher standard deviation of RMSE at *numsamples* values of 4 and lower and *samplesize* values of 4000 ha^{-1} and lower. For the test area this leads to the conclusion that the optimal *numsamples* and *samplesize* values considering both the DTM quality and the expected stability of the DTM quality are 10,000 ha^{-1} and 4, respectively. However, near optimal values can already be obtained with 7000 points per ha and 3 iterations. In an operational setting, the *samplesize* value for the test area would be between 4000 ha^{-1} and 10,000 ha^{-1}, depending on the desired balance between DTM quality and computational cost.

Table 1
RMSE values in meters for the filtering with the morphological filtering

Slope of filter kernel	RMSE w.r.t. visually filtered ground points	RMSE w.r.t. field measured ground points	Average residual w.r.t. field measured ground points	Output number of ground points per hectare
30°	0.34	1.79	−0.96	12,970
40°	0.20	0.79	−0.22	28,506
50°	0.13	0.41	0.06	35,708
60°	0.14	0.28	0.17	38,455
70°	0.14	0.30	0.19	39,208
REIN	0.16	0.25	0.22	n.a.

The values for REIN (at samplesize = 10,000 and numsamples = 4) are shown for comparison.

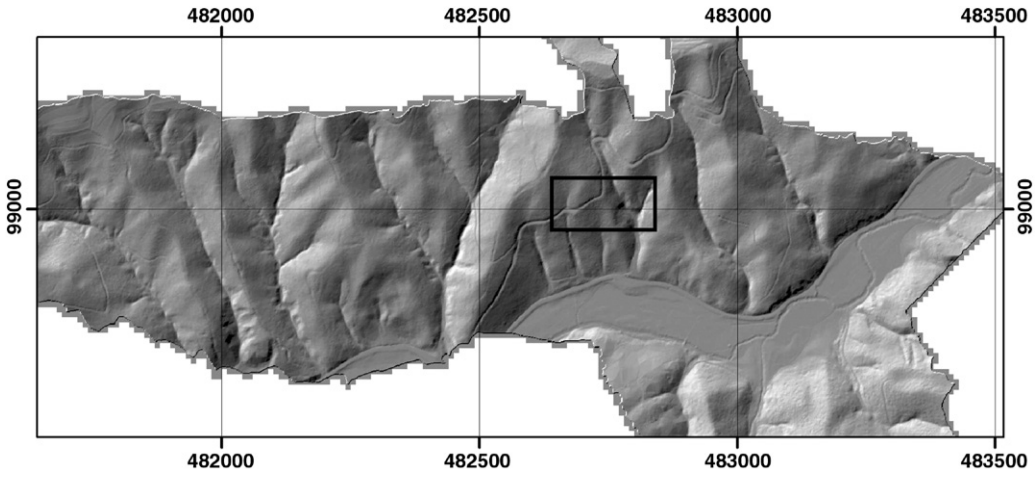

Fig. 6. The DTM of the entire scanned area (1179 ha) was produced with REIN, of which a subset is shown here, corresponding with the DSM and aerial ortho-photo shown in Fig. 3a and b, respectively. The small rectangle shows the location of the test area.

Analysis based on the field measured ground points yields the same values of *numsamples* and *samplesize* for optimal results, but the average RMSE are approximately 50% larger (Section 5.3). This assures that the transects placement did not have a large impact on the parameter selection.

No dependence of average RMSE on relief slope and canopy cover was found in the test area.

Filtering the area shown in Fig. 3a with REIN results in the DTM shown in Fig. 6. The area comprises flat, moderately sloped, and steep forested regions as well as regions without vegetation. Slopes, including the very steep areas, are maintained entirely. Also structures such as forest roads and river embankments are maintained, whereas obvious filter errors are minimal as presented in Fig. 4h.

5.2. Comparison to morphological filtering

The proposed algorithm was compared to the morphological filtering as specified by Vosselman (2000). The filter kernel was defined with a constant offset of ±53 cm, considering the vertical measurement error of the difference of two measured elevations, and admissible slopes between ground points with values of 30° to 70° in steps of 10°. These slopes cover the range from the average slope to the extreme slopes in the test area. The filter radius was set to 10 m. The resulting point clouds were triangulated to produce DTMs. In Table 1 the RMSE values with respect to the visually filtered point cloud and the field measured ground points are shown. The number of identified ground points grows strongly for slopes from 30° to 60°, because many ground points in steeper areas are incorrectly removed using too low kernel slopes. Areas of high slopes are essentially chopped off and replaced by (large) triangles of the final TIN (Fig. 4b), which explains the negative average residuals for low kernel slopes. This artifact vanishes for slopes larger than 70° (Fig. 4c), but vegetation points still remain in the filtered data set. Such result is expected, because the morphological filter is a general purpose filter, whereas the filter presented here is designed for natural, possibly forested, areas and not, e.g., for built-up city areas. The RMSE values are comparable to the results of REIN and with ±14 cm even slightly lower for the morphological filtering. Fig. 4c, however, shows that the number of artifacts, i.e. remaining hills from vegetation points, is much higher in the morphological filter results than in the optimal REIN example. As with the slope filtering results, the transects of visually identified points apparently by-pass most of the artifacts in morphologically filtered DTM. The measured field points, on the other hand, are spread more evenly and show a higher error for the morphological filtering than for REIN.

5.3. Assessment of REIN based on the field measured ground points

To assess the overall performance of the proposed algorithm and the given data, the points measured with total station were compared to the DTM computed with REIN and the DTMs obtained from morphological filtering (Table 1).

In Table 1, the parameters chosen for REIN are those as described in Section 5.1, i.e., 10,000 points per ha and 4 iterations. These values are not only optimal when comparing to the visually identified points, but also optimal when comparing to the field measured ground points. For REIN the RMSE is ±25 cm (compared to ±16 cm for the check against the visually identified ground points), the extremes are −84 cm and +97 cm and the mean value of the residuals is +21.5 cm, indicating that the laser points lie higher than the tachymetrically measured points in this area. This observation is also supported by the analysis of the morphological filtering (Table 1, column showing average residuals).

Possible explanation for the offset within the REIN algorithm is an exceedingly high value of gmo, but as a similar height shift is also observed for the morphological filter results, this is excluded. Also the removal process for negative outliers cannot explain that upward shift. In fact, the average height of the removed points is 15 cm above the DTM computed with REIN, which indicates that the removal process was too strict because too many real ground points were removed, too. Comparing all points, i.e. also those marked as negative outliers, to the DTM shows that the point with the largest negative distance to the DTM is 0.91 m below. The 0.2% of points with the largest negative distances reach up to 45 cm below the terrain, which is in the same order as the precision derived above.

The offset can, however, be explained by the measurement characteristics of laser scanning. Over steep ground an upward shift is observed in the measured points because the echo detection techniques in the receiver favor the rising edge of the backscattered signal, which is coming from the higher region within the footprint. Also the herbaceous vegetation causes an offset of the points as the reflection of the laser energy is performed, at least partly, by the leaves a few cm above the ground.[5] An error in geo-referencing cannot be excluded, either, but is not necessary for explaining the effect.

Reducing the lidar point elevations by the mean value reduces the RMSE to ±20 cm for REIN. This value has to be split into three vertical components: the total station measurement accuracy (±9 cm, Section 4), the lidar point accuracy (±38 cm, Section 4), and the ground point selection accuracy (±15 cm, which is the RMSE with reference to the visually identified ground points). Adding these three accuracy figures quadratically amounts to ±42 cm, which is much higher than the accuracy of ±20 cm for REIN after subtracting the offset. Obviously, not all of these errors are purely random, i.e. different for each point, which would justify adding them quadratically. Some of these errors are therefore systematic, in the sense of “similar for neighboring points”. The random component of the lidar point accuracy may therefore be below ± 20 cm within the investigated area.

[5] Overviews on echo detection methods and impacts thereof are discussed e.g. in Jutzi and Stilla, 2003; Fox et al., 1993; Hopkinson et al., 2004; Pfeifer et al., 2004.

Summarizing, REIN provides on the sample data a ground point classification of ±16 cm (obtained from the comparison to visual identified ground points) and a DTM accuracy of ±20 cm.

6. Summary and conclusions

We presented the repetitive interpolation (REIN) method for DTM computation from the raw airborne laser scanning point cloud. It is especially applicable in steep, forested areas where other filtering algorithms typically have problems distinguishing between ground returns and off-ground points reflected in the vegetation. The REIN algorithm is applied after initial filtering, which involves the removal of all negative outliers and the removal of most, but not necessarily all, off-ground points (positive outliers) by some existing filtering algorithm, for instance the morphological filter. The core idea of the REIN algorithm is to make use of the redundancy in the initially filtered point cloud FPC in order to mitigate the effect of the residual off-ground points. Multiple independent samples are taken from the FPC, while each part of the area of interest gets equal probability of being sampled, irrespective of the local ground return density. Based on each sample, ground elevation estimates are computed at individual DTM locations, using some spatial interpolation method, for instance TIN based interpolation. Because the lower bounds of the distributions of the elevation estimates at each DTM location are almost insensitive to positive outliers, the true ground elevations can be approximated by adding the global mean offset to the lower bounds of distributions. Assuming that relatively few off-ground points remained in the FPC, the global mean offset can be estimated over all DTM locations by averaging the offsets of all elevation estimates to the lower bounds of their respective elevation distributions.

The performance of REIN was tested in an area of steep relief covered by mixed forest, the influence of sample size and number of samples (i.e., iterations) on DTM quality was analyzed, and a baseline DTM (i.e., without REIN) and a morphologicaly filtered DTM were computed for comparison. Using REIN, the obtained global root mean square elevation error values ranged between ± 0.16 m and ±0.37 m, depending on the sample size and number of samples. The lowest error of ±0.16 m was achieved with 4 samples and using a 23% sampling rate. A standard method was applied to the data and the filtering error reached in the best case ±3.2 m. Comparison to ground points measured with a total station showed a vertical offset of 20 cm, i.e., the lidar points were lying above the ground. Straightforward computation of residuals showed an overall error of ±0.28 m which includes the main components of laser measurement accuracy and ground point selection accuracy. Considering the 20 cm offset, the root mean square error of the lidar DTM computed with REIN, is reduced to ±0.20 m.

While REIN uses random sampling to select lidar points in each iteration, it also ensures that each part of the area of interest gets equal probability of being sampled, irrespective of the local ground return density. These properties enable REIN to deal with sparse ground returns under dense forest canopy on one hand, but also with highly redundant ground returns in forest openings on the other. It results in a homogeneous DTM even under non-homogeneous data input conditions. The problem of negative outliers, originating from multi path reflections, is also addressed in the preprocessing step of the REIN method. The random sampling makes REIN unique among the methods of filtering airborne laser data. Other filters behave deterministically, always generating a filter error in special situations. Because of its random aspects, these errors do not occur in each sample taken during REIN and typically cancel out in the final step of computing final elevations at the DTM points. REIN has thus a greater ability to adapt to variations in the terrain.

The final DTM is not biased towards the lowest elevation estimates, because the final elevation at each DTM location is computed by adding the global mean offset to the lowest elevation at each DTM location.

REIN does not impose a certain DTM data structure. It can accommodate either DTM as a regular vector grid or as a TIN. A data structure that includes break lines is favoured. Concerning break lines the presented filter algorithm behaves like other presented algorithms, i.e., inducing a small round off. Break lines should be extracted by a separate process and stored explicitly. Furthermore, REIN operates by interpolating DTMs from several independent samples of lidar points. This enables a straightforward parallelization of REIN, potentially leading to a considerable reduction of processing time.

In further work, more complex estimators for the offset, other than the mean value could be considered, e.g., by incorporating additional knowledge on the influence of low herbaceous vegetation on airborne laser scanning. Further tests of REIN are needed to get a better assessment of its performance in different forest types and under various scanning conditions. A new study at the Slovenian Forestry Institute is studying the influence of point density. In the future we will also concentrate on a method of automated optimization of REIN parameter values and on applications of REIN in the forestry domain. As the work has shown, also the problem of negative outliers, should be studied further. The REIN-based DTM could enable a more accurate DSM normalization in a very steep and eroded terrain, and implicitly also detailed vegetation height analyses in some geomorphologically specific habitats, e.g., in narrow karstic dolines and sinkholes.

Acknowledgements

The authors would like to thank Polona Kalan, Slovenian Forestry Institute, and George Sithole, TU Delft, for fruitful discussions of the algorithm. We owe special thanks to ELES company, Slovenia, for kindly giving us the lidar data of the test area. The study was funded by the Slovenian Research Agency and by the Slovenian Ministry of Agriculture, Forestry, and Food within the research project “Processing of Lidar Data” (contract 3311-04-8226575), and by the Slovenian Ministry of Defense and by the Slovenian Research Agency within the research project “Forecasting GIS Model of Fire Danger in Natural Environment” (contract 3311-04-828032). We are grateful for the support of Prof. Vosselman, ITC Enschede, by providing executables for the standard method of filtering ALS data with morphological filtering.

Appendix A. The REIN algorithm

```
# Inputs:
#    FPC — list of filtered (3-D) LiDAR points
#    DTMxy – list of points in the X–Y plane (2-D) we want to include in DTM
#    num_samples — number of iterations (samples)
#    sample_size — number of points in each sample
#
# Output:
#    DTM — digital terrain model providing elevation for each point in DTMxy
#
# Time complexity of the algorithm governed by performing Delaunay triangulation (DT)
# is O(num_samples * sample_size * log sample_size)

function ComputeDTM(FPC, DTMxy, num_samples, sample_size)

    # for each point in DTMxy…
    foreach (x,y) in DTMxy do
       EE[x,y] = empty list

    # … collect elevations estimated (EE) on different samples taken from FPC
    iteration = 1
    while iteration <= num_samples do
        FPCs = GetSample(FPC, sample_size)
        DT = GenerateDT(FPCs)
        foreach (x,y) in DTMxy do
            Zest = ElevationDT(DT, (x,y))
            append Zest to EE[x,y]
        iteration = iteration +1

    # based on elevations calculate global mean offset (gmo)
    OS = empty list
    foreach (x,y) in DTMxy do
        offset = Mean(EE[x,y]) — Min(EE[x,y])
        append offset to OS
    gmo = Mean(OS)

    # using estimated elevations and gmo, calculate digital terrain model DTM
    DTM = empty list
    foreach (x,y) in DTMxy do
        z = Min(EE[x,y]) + gmo
        append (x, y, z) to DTM
    return DTM
# Inputs:
#    FPC — list of filtered LiDAR points
#    sample_size — number of points in each sample
#
# Output:
#       FSP — list of sample_size randomly selected points from FPC

function GetSample(FPC, sample_size)

        FSP = empty list
        while Length(FSP) < sample_size do
            (x,y) = random point uniformly distributed over X–Y projection of FPC
            find (x_S,y_S,z_S) in FPC that is closest to (x,y) in the X–Y plane
            if (x_S,y_S,z_S) not in FSP
                append (x_S,y_S,z_S) to FSP
        return FSP

# Input:
#       P — list of points
#
# Output:
#       DT — Delaunay triangulation over the points in P
```

Appendix A (*continued*)

```
function GenerateDT(P)

# implemented using the Triangle software package available at
# http://www-2.cs.cmu.edu/~quake/triangle.html
    return DT

# Input:
#       DT — Delaunay triangulation
#       (x,y) — a point
#
# Output:
#       zest — estimated elevation of (x,y) according to DT

function ElevationDT(DT, (x,y))

    find triangle T in DT such that (x,y) is within the X–Y projection of T
    zest = elevation of the plane defined by T at (x,y)
    return zest
```

References

Andersen, H. -E., McGaughey, R., Carson, W., Reutebuch, S., Mercer, B., & Allan, J. (2004). A comparison of forest canopy models derived from lidar and InSAR data in a pacific northwest conifer forest. *International Archives of Photogrammetry and Remote Sensing*, *35*(B3) (Istanbul, Turkey).

Axelsson, P. (2000). DEM generation from laser scanner data using adaptive TIN models. *International Archives of Photogrammetry and Remote Sensing*, *33*(B4/1), 110−117 (Istanbul, Turkey).

Blair, J., Rabine, D., & Hofton, M. (1999). The Laser Vegetation Imaging Sensor: A medium-altitude, digitisation-only, airborne laser altimeter for mapping vegetation and topography. *ISPRS Journal of Photogrammetry and Remote Sensing*, *54*, 115−122.

Bufton, J. (1989). Laser altimetry measurements from aircraft and spacecraft. *Proceedings IEEE*, *Vol. 70* (pp. 463–477).

Elmqvist, M. (2001). *Ground estimation of lasar radar data using active shape models.* OEEPE workshop on airborne laser scanning and interferometric SAR for detailed digital elevation models, Stockholm, Sweden.

Fox, C. S., Accetta, J. S., & Shumaker, D. L. (1993). *Active electro-optical systems, Vol 6, of The infrared and electro-optical system handbook.* SPIE Optical Enginnering Press.

Haralick, R. M., & Shapiro, L. G. (1992). *Computer and Robot Vision*, *Vol. I.* Reading, MA: Addison Wesley.

Hjaltason, G. R., & Samet, H. (1995). Ranking in spatial databases. In Egenhofer & Herring (Eds.), *Lecture notes in computer science*, *Vol. 951* (pp. 83–95). Berlin: Springer-Verlag.

Hopkinson, C., Lim, K., Chasmer, L. E., Treitz, P., Creed, I. F., & Gynan, C. (2004). Wetland grass to plantation forest — Estimating vegetation height from the standard deviation of lidar frequency distributions. *International Archives of Photogrammetry and Remote Sensing*, *36*(8W2), 288−294 (Freiburg, Germany).

Hyyppä, J., Hyyppä, H., Litkey, P., Yu, X., Haggrén, H., Rönnholm, P., et al. (2004). Algorithms and methods of airborne laser-scanning for forest measurements. *International Archives of Photogrammetry and Remote Sensing*, *36*(8/W2) (Freiburg, Germany).

Ip, A., El-Sheimy, N., & Hutton, J. (2004). Performance analysis of integrated sensor orientation. *International Archives of Photogrammetry and Remote Sensing*, *35*(B5) (Istanbul, Turkey).

Jacobsen, K., & Lohmann, P. (2003). Segmented filtering of laser scanner DSMs. *International Archives of Photogrammetry and Remote Sensing*, *34* (3/W13) (Dresden, Germany).

Jutzi, B., & Stilla, U. (2003). Analysis of laser pulses for gaining surface features of urban objects. *2nd GRSS/ISPRS Joint Workshop on Remote Sensing and Data Fusion of Urban Objects, URBAN 2003, IEEE* (pp. 13−17).

Kaartinen, H., et al. (2005). Accuracy of 3D city models: EuroSDR comparison. *International Archives of Photogrammetry and Remote Sensing*, *Vol. 36, 3/W19*. The Netherlands: Enschede.

Kass, M., Witkin, A., et al. (1988). Snakes: Active contour models. *International Journal of Computer Vision*, *1*, 321−331.

Kilian, J., Haala, N., & Englich, M. (1996). Capture and evaluation of airborne laser data. *International Archives of Photogrammetry and Remote Sensing*, *31*(3), 383−388 (Vienna, Austria).

Kraus, K., & Pfeifer, N. (1998). Determination of terrain models in wooded areas with airborne laser scanner data. *ISPRS Journal of Photogrammetry and Remote Sensing*, *53*, 193−203.

Lohmann, P., Koch, A., & Schaeffer, M. (2000). Approaches to the filtering of laser scanner data. *International Archives of Photogrammetry and Remote Sensing*, *33*(B3/1), 534−541.

Measures, R. M. (1992). *Laser remote sensing: Fundamentals and applications.* Malabar, Fla: Krieger Pub.

Nardinocchi, C., Forlani, G., & Zingaretti, P. (2003). Classification and filtering of laser data. *International Archives of Photogrammetry and Remote Sensing*, *34*(3W13) (Dresden, Germany).

Pfeifer, N., Gorte, B., & Oude Elberink, S. (2004). Influences of vegetation on laser altimetry — Analysis and correction approaches. *International Archives of Photogrammetry and Remote Sensing*, *36*(8W2), 283−287 (Freiburg, Germany).

Pfeifer, N., Stadler, P., & Briese, C. (2001). *Derivation of digital terrain models in the SCOP++ environment.* OEEPE workshop on airborne laserscanning and interferometric SAR for detailed digital elevation models, Stockholm, Sweden.

Samet, H. (1984). The Quadtree and related hierarchical data structures. *ACM Computing Surveys (CSUR)*, *16/2*, 187−260.

Schiewe, J. (2001). Ein regionen-basiertes Verfahren zur Extraktion der Geländeoberfläche aus Digitalen Oberflächen-Modellen. *Photogrammetrie, Fernerkundung, Geoinformation*, *2*, 81−90.

Shewchuk, J. R. (2005). Triangle: A two-dimensional quality mesh generator and Delaunay triangulator. http://www.cs.cmu.edu/~quake/triangle.html, last accessed September 29, 2005.

Sithole, G. (2001). Filtering of laser altimetry data using a slope adaptive filter. *International Archives of Photogrammetry and Remote Sensing*, *34*(3/W4), 203−210 (Annapolis, ML).

Sithole, G. (2005). Segmentation and Classification of Airborne Laser Scanner Data, Dissertation, TU Delft, ISBN 90 6132 292 8, Publications on Geodesy of the Netherlands Commission of Geodesy, Vol. 59.

Sithole, G., & Vosselman, G. (2004). Experimental comparison of filter algorithms for bare—Earth extraction from airborne laser scanning point clouds. *ISPRS Journal of Photogrammetry and Remote Sensing*, *59*, 85−101.

Sohn, G., & Dowman, I. (2002). Terrain surface reconstruction by the use of tetrahedron model with the MDL criterion. *International Archives of Photogrammetry and Remote Sensing*, *34*(3A), 336−344 (Graz, Austria).

von Hansen, W., & Voegtle, T. (1999). Extraktion der Geländeoberfläche aus flugzeuggetragenen Laserscanner-Aufnahmen. *Photogrammetrie, Fernerkundung, Geoinformation*, *4*, 229−236.

Vosselman, G. (2000). Slope based filtering of laser altimetry data. *International Archives of Photogrammetry and Remote Sensing*, *Vol. 33, B3/2* (pp. 935–942). The Netherlands: Amsterdam.

Wagner, W., Ullrich, A., Ducic, V., Melzer, T., & Studnicka, N. (2006). Gaussian decomposition and calibration of a novel small-footprint full-waveform digitising airborne laser scanner. *ISPRS Journal of Photogrammetry and Remote Sensing*, *60*, 100−112.

Zakšek, K., & Pfeifer, N. (2006). An improved morphological filter for selecting relief points from a LIDAR point cloud in steep areas with dense vegetation. *Technical Report, Institute of Anthropological and Spatial Studies, Solvenia.* http://iaps.zrc-sazu.si/files/File/Publikacije/Zaksek_Pfeifer_ImprMF.pdf, accessed 6.6.2006.

Zhang, K., Chen, S., Whitman, D., Shyu, M., Yan, J., & Zhang, C. (2003). A progressive morphological filter for removing nonground measurements from airborne LIDAR data. *IEEE Transactions on Geoscience and Remote Sensing*, *41*(4), 872−882.

Zwally, J., et al. (2002). ICESat's laser measurements of polar ice, atmosphere, ocean, and land. *Journal of Geodynamics*, *34*, 405−445.